

Development, Optimization and Evaluation of Silver Sulphadiazine Loaded Nanofibrous Scaffold as Wound Dressing

Reshma Thampy*

Department of Science, Indian Institute of Science Education and Research, Pune, Maharashtra, India

*Corresponding author: Reshma Thampy, Department of Science, Indian Institute of Science Education and Research, Pune, Maharashtra, India, Tel: 95362705203; E-mail: reshmathampy421@gmail.com

Received date: September 26, 2020, Manuscript No. IJDDR-20-6229; Editor assigned date: September 29, 2020, PreQC No. IJDDR-20-6229 (PQ); Reviewed date: November 26, 2020, QC No. IJDDR-20-6229 Revised date: October 13, 2022, Manuscript No. IJDDR-20-6229 (R); Published date: October 26, 2022, DOI: 10.36648/0975-9344.22.14.978

Citation: Thampy R (2022) Development, Optimization and Evaluation of Silver Sulphadiazine Loaded Nanofibrous Scaffold as Wound Dressing. Int J Drug Dev Res Vol:14 No:10

Abstract

The aim of the study was to design, optimize and evaluate silver sulphadiazine loaded nanofibrous scaffold as wound dressing. In this research medicated biodegradable polymeric scaffolds are prepared which works both as anti-infective dressing and proactive. The potential of using the intact skin as port of drug administration has been recognized for several decades. Transdermal therapeutic systems have been designed to provide controlled continuous delivery of drugs *via* the skin to the systemic circulation. The formulation was optimized by factorial design (design expert software) with polymer solution ratio, voltage, distance as the factor and diameter of nanofiber, cumulative drug release at 7th day, biodegradability rate at 10th day as responses. The optimized formulation containing diameter of nanofiber 78.38 nm, cumulative drug release at 7th day 97.79%, biodegradation rate at 10th day 85.76%.

Keywords: Silver sulphadiazine; Wound healing; Nanofibrous scaffold; Optimization

Introduction

Wound healing is an intricate process whereby the skin (or another organ tissue) repairs itself after injury and the wounds may get infected [1]. To prevent infection, we can use different wound healing medicaments including antibiotics. Wound dressings protect the wound from external environment by covering the wounds.

Chronic non healing wounds show delayed and incomplete healing processes and in turn expose patients to a high risk of infection. Treatment currently focuses on dressings that prevent microbial infiltration and keep a balanced moisture and gas exchange environment. Antibacterial delivery from dressings has existed for some time, with responsive systems now aiming to trigger release only if infection occurs. Simultaneously, approaches that stimulate cell proliferation in the wound and encourage healing have been developed [2]. Interestingly, few dressings appear capable of simultaneously treating infection

and encouraging cell proliferation/wound healing. Electro spinning is a simple, cost-effective, and reproducible process that can utilize both synthetic and natural polymers to address these specific wound challenges. Electro spun meshes provide high surface area, micro-porosity, and the ability to load drugs or other biomolecules into the fibers. Electro spun materials have been used as scaffolds for tissue engineering for a number of years, but there is surprisingly little literature on the interactions of fibers with bacteria and co cultures of cells and bacteria. And the research that is required to develop smart multifunctional wound dressings capable of treating infection and healing chronic wounds [3].

Materials and Methods

Silver sulphadiazine was obtained Galentic India Pvt. Ltd (Mumbai), lysozyme was obtained from Yarrow Chem Pvt. Ltd, (Mumbai). Sodium alginate, polyvinyl alcohol, ammonia solution and other solvents are purchased from nice chemicals, Kochi [4]. All other materials used in studies were of analytical grade and were used as received.

Preformulation Studies

Identification of drug

Identification by FTIR spectroscopy: Drug was identified using FTIR spectroscopy. The FTIR spectrum of the obtained drug sample was compared with that of standard FTIR spectrum for functional group of the pure silver sulphadiazine.

Identification by melting point: Melting point of pure Silver sulphadiazine was determined using open capillary method. The capillary tube fused at one end was filled with the drug sample by repeated tapings [5]. The capillary tube was then placed in a Thiele's melting point apparatus. The temperature at which the drug started to melt was recorded. This was performed thrice and the average value was calculated.

Physicochemical properties of the drug

Organoleptic properties: The physical appearance of drug was observed and compared with the pharmacopoeial specifications.

Solubility study: Solubility of drug was observed in different solvents such as water, chloroform, methanol, ethanol and Ammonia solution.

Analytical methods

Determination of λ_{\max} of silver sulphadiazine: The λ_{\max} of silver sulfadiazine was determined in PBS pH 7.4. Silver sulfadiazine was dissolved in ammonia solution and the UV absorption spectra were taken after suitable dilutions with respective media [6]. The wavelength, which showed maximum absorption, was taken as the λ_{\max} of the drug with respect to that media.

Preparation of calibration curve of silver sulphadiazine: Accurately weighed 10 mg of silver sulfadiazine was transferred to a 100 ml volumetric flask and dissolved in 0.5 ml of ammonia solution. The volume was adjusted to the mark with distilled water to prepare stock solution (100 $\mu\text{g}/\text{ml}$). The above stock solution (100 $\mu\text{g}/\text{ml}$) was further diluted with distilled water to get concentration of silver sulfadiazine in the range of 1-10 $\mu\text{g}/\text{ml}$ [7]. Absorbance of each solution was measured at 254.0 nm against a reagent blank solution prepared similarly without drug using Shimadzu 1800 UV/Visible double beam spectrophotometer. Calibration curve was prepared by plotting

concentration versus absorbance. Similar calibration curves were also prepared for Silver sulfadiazine in PBS pH 7.4 and the absorbances were recorded at 254 nm respectively.

Fabrication of medicated nanofibrous scaffold

Preparation of the polymer solutions: Preparation of 2% sodium alginate solution 2% sodium alginate solution was prepared by adding 2 grams of sodium alginate powder into 100 ml of purified water with constant agitation for 4 h at room temperature.

Preparation of 10% PVA solution: 10% PVA solution was prepared by dissolving 10 grams of PVA into 100 ml of purified water at 60°C baths with gentle magnetic stirring for 4 h.

Preparation of blend: The above solutions of Sodium alginate and PVA were mixed in the volume ratios of 65/35, 75/25 and 70/30 separately. Calculated quantity of Silver sulfadiazine dissolved in minimal quantity of ammonia solution was added to the blend so as to contain 1% drug to the dry polymer weight. The blend was stirred continuously for 2 h at room temperature for proper mixing and internal binding in the solution (Table 1) [8].

Table 1: preparation of the polymer solution.

Volume ratio (PVA: Sodium alginate)	Amount of dry PVA (grams)	Amount of dry sodium alginate (grams)	Amount of drug to contain 1% (grams)
75:25	7.5	0.5	0.08
70:30	7	0.6	0.076
65:35	6.5	0.7	0.072

Electro spinning of the prepared solutions

The solution was loaded into the plastic syringe (10 ml) and this was placed inside the electro spinning machine espin nano. A blunt ended 22 gauge stainless steel needle was connected to the syringe which acted as the nozzle [9]. The emitting electrode from a gamma high voltage research ES30P power supply capable of generating DC voltages up to 30 kV was attached to the needle. The grounding electrode from the same power supply was attached to a rectangular piece of aluminium foil which acted as collector plate. Upon application of a high voltage ranging between 15-30 kV across the needle and the collector plate, a fluid jet was initiated from the nozzle and accelerated towards the collector. The solvent gradually evaporated, leaving only ultrathin fibers on the collector. As this process continued for a considerable time period, the deposited fiber turns to a thin film. The obtained nanofibrous scaffold was left exposed to air for complete drying (Figure 1) [10].



Figure 1: Espin-nano (electrospinning machine).

Selection of range of critical parameters for optimization: Number of trials was run to identify the critical parameters which could affect the diameter of fiber, biodegradability and drug release [11]. The factors varied during the trial were polymer ratio, tip to collector distance and voltage. Based on the fiber diameter, the polymer solution ratio was fixed at 65/35, 70/30 and 75/25. Similarly the voltage was fixed at 17, 20 and 23 kV. The tip to collector distance was kept at 20, 24 and 28 cm.

Cross linking of sodium alginate/PVA/nanofibrous scaffold: As both Sodium alginate and PVA are readily soluble in water, their hydrophilic property should be reduced for its prolonged use as wound protective film and drug depot. The fibrous

scaffold were first treated with 2% glutaraldehyde vapor in a desiccator for 48 h and then dipped in 1% CaCl₂ in ethanol for 1 h in order to crosslink the polymer thereby decrease their hydrophilic property. Glutaraldehyde is a universal cross linking

agent for polymers and calcium chloride is react with sodium alginate to form insoluble calcium alginate [12]. The cross linked nano fibers were then dipped in water for 48 h to confirm their water insoluble nature (Table 2).

Table 2: Formulation table for the medicated nanofibrous scaffold as per the factorial (adjusted) design.

Sl. No	Formulation code	Polymer solution ratio (PVA:SA) (coded)	Voltage (coded)	Distance (coded)	Polymer solution ratio (PVA:SA)	Voltage (kV)	Distance (cm)
1	F1	1	-1	-1	75:25	17	20
2	F2	1	1	1	75:25	23	28
3	F3	-1	1	-1	65:35	23	20
4	F4	-1	-1	1	65:35	17	28
5	F5	-1	-1	-1	65:35	17	20
6	F6	-1	1	1	65:35	23	28
7	F7	1	1	-1	75:25	23	20
8	F8	1	-1	1	75:25	17	28
9	F9	0	0	0	70:30	20	24
10	F10	0	0	0	70:30	20	24
11	F11	0	0	0	70:30	20	24
12	F12	0	0	0	70:30	20	24

Evaluations of the medicated nanofibrous scaffold

Nanofiber formulations were evaluated and characterized by the following methods.

Physical appearance: All the nanofibrous scaffold were visually inspected for color, clarity, flexibility and smoothness.

Morphological characterization by SEM analysis: Fiber morphology, texture and dimensions of the fibers were studied using scanning electron microscope with an accelerating voltage of 20 kV. Obtained images were analyzed using Image J software for the calculation of the average diameter of the nano fibers [13]. A Scanning Electron Microscope (SEM) is a kind of electron microscope which produces images of a sample by scanning it with a focused beam of electrons. The electrons from the machine interact with electrons in the sample, producing various signals that are detected and thus we get information regarding the sample's surface topography and composition. For SEM analysis, a small piece of sample was taken which is given a platinum coating and then it is placed on the SEM multi holder [14]. It was then inserted into the chamber and on application of high accelerating voltage, SEM images were obtained.

Determination of porosity: The porosity was determined using image analysis algorithms by MATLAB (Math Works,

Version 7) based on global thresholding method. According to the global thresholding, the binary images were created and a single constant threshold was used to segment the images. All pixels up to and equal to the threshold were considered the object and the remaining ones were belonged to the background. Percent of porosity was determined [15].

$$P = \left(1 - \frac{n}{N}\right) \times 100$$

Where, 'n' is number of white pixels, 'N' is total number of pixels in image and 'P' is percent of porosity.

Swelling index: Degree of swelling represents the relative measure of the cross linking between the nano fibers. The swelling index of drug loaded nanofibrous scaffold was determined in phosphate buffer (pH 7.4) at room temperature [16]. The swollen weight of the nanofiber was determined at predefined time intervals. The swelling index was calculated by the following equation:

$$\text{swelling index} = \frac{W_t - W_0}{W_0}$$

Where 'W_t' is the weight of swollen nanofiber at time 't' 'W₀' is the weight of dried nanofiber.

Drug content estimation: Nano fibers were cut into 2 × 2 cm and taken in a 100 ml standard flask. Dissolved the contents in ammonia solution and made up to the volume with distilled water and subjected to continuous shaking in a shaker for 3 hours. After proper dilution, the absorbance was measured at 254 nm using a UV visible spectrophotometer.

$$\text{Percentage drug content} = \frac{\text{Practical content} \times 100}{\text{Theoretical content}}$$

Biodegradability test: The *in vitro* degradation of medicated nano fibers (2 x 2 cm) was carried out in 1 ml phosphate buffer

solution (PBS, PH 7.4) at 37°C containing 1.5 µg/ml lysozyme .The concentration of enzyme was chosen to correspond to the concentration in the human serum. Briefly nano fibers of known dry weights were sterilized by autoclaving (120°C, 20 min) and incubated in the lysozyme solution with gentle mechanical agitation during the period of study. The lysozyme solution was refreshed daily to ensure continuous enzyme activity. The samples were withdrawn at definite time intervals from the medium, rinsed with distilled water, dried under vacuum and weighed [17]. The *in vitro* degradation was expressed as percentage of weight loss of the dried nano fibers on every alternate day during the lysozyme treatment. To separate between enzymatic degradation and dissolution, control samples were stored under the same conditions as described above, but without the addition of lysozyme (Table 3).

Optimization by factorial designs

Table 3: List of factors and responses with their levels and constraints.

Factors	Levels used		
	-1	0	1
X ₁ =Polymer solution ratio	65:35:00	70:30:00	75:25:00
X ₂ =Voltage (kV)	17	20	23
X ₃ =Distance (cm)	20	24	28
Responses	Constraints		
Y ₁ =Diameter of nanofiber (nm)	70-100 nm		
Y ₂ =Cumulative drug release at 7 th day (%)	85-95%		
Y ₃ =Biodegradability rate at 10 th day (%)	75-86%		

Development of the optimum batch

Based on the above data, an optimum formula was suggested by the statistical software design expert 10.0.3.1 trial version.

The batch was then prepared in the same way as before (Table 4).

Table 4: Optimum formula.

Polymer solution ratio (PVA: SA)	Voltage (kV)	Distance (cm)	Diameter of nanofiber (nm)	Cumulative drug release at 7 th day (%)	Biodegradation rate at 10 th day (%)
65:35	17.027	27.94	78.38	97.79	85.76

Evaluations of the optimum formula

The prepared optimum formula suggested by the software was evaluated for various parameters like, physical appearance, morphological characterization by SEM, XRD analysis, TGA analysis, percentage swelling Index, drug content estimation,

biodegradability test, *in vivo* wound healing and stability studies [18].

X-Ray Diffraction (XRD): X-ray crystallography is a method used for determining the atomic and molecular structure of a crystal. The crystalline atoms cause a beam of X-rays to diffract into many specific directions and these diffracted rays give an

idea about the crystalline structure of the molecule. Blended polymeric nanofibers were analyzed using X-ray Diffractometer (Bruker AXS D8 Advance). Samples were scanned for full XRD patterns from 3.00°C-80.00°C 2θ with step size 2°/min at 30 kV tension and 20 mA current.

Thermo Gravimetric Analysis (TGA): Thermo Gravimetric Analysis (TGA) was used to measure the amount and rate of change in the weight of a material as a function of temperature in a controlled atmosphere. 5 mg of nanofiber was used to study thermo gravimetric behavior using an automatic thermal analyzer system (Diamond TG/DTA 8.0, Perkin-Elmer, USA) [19]. Samples were crimped in standard aluminum pans and heated from 35° to 700°C at a heating rate of 10°C/min under constant purging of dry nitrogen at 20 ml/min. An empty pan, sealed in the same way as the sample, was used as a reference. The graph was plotted with weight (percentage) vs. temperatures.

Table 5: Design of experimental groups.

Group	Treatment
1	Control-untreated
2	Standard (1% silvadene cream)
3	Formulation (medicated nanofiber)

Wound healing evaluation parameters

Wound contraction measurement: The wound contractions were measured as the percentage of wound reduction in the wound area measured every 2 days after wound formation [21]. For wound size measurement, the wounds were traced on a transparency paper and the tracings were measured. The reduction in the wound size was calculated by the formula:

$$W\% = [(WA_0 - WA_t) / WA_0] \times 100$$

Where, W% is the percentage of wound healing,

WA₀ is the area of wound at 0th day and

WA_t is the area of wound after different days of healing.

Epithelialization period: Epithelialization period was monitored by noting numbers of days required for the Escher to fall off from the wound surface without leaving a raw wound behind. The epithelialization period was measured from initial day.

Stability studies: The stability studies were carried out on the optimized formulation of nanofibrous scaffold at room temperature over a period of 60 days. Folding endurance, % drug entrapment and *in vitro* drug release were evaluated before and after the stability study (Figure 2, Tables 6 and 7).

In vivo study for wound healing activity

Excision wound model: Wound healing study was carried out as per the guidelines and the approval of institutional animal ethical committee as given previously. A small area on the dorsal cervical region of the albino rats were shaved, wiped with alcohol, anesthetized with ketamine hydrochloride injection and a 2 cm diameter full thickness skin excision was made at three sites. The medicated nanofibrous scaffold with same dimension was applied on the wound at one site. The second wound was treated with the Silver sulphadiazine 1% cream (Solpadine) once every day as positive control and the third was kept bare as negative controls [20]. The photographs were taken each day until the wounds were perfectly healed. In this model wound contraction and epithelialization period was also monitored (Table 5).

Results and Discussion

Preformulation Studies

Identification of drug

FTIR spectroscopy:

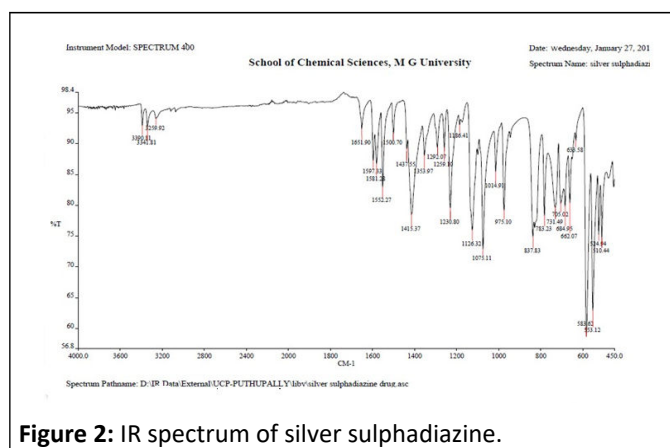


Figure 2: IR spectrum of silver sulphadiazine.

Table 6: Interpretation of IR spectrum of silver sulphadiazine.

Functional group	Characteristic peaks (cm ⁻¹)	Observed peak (cm ⁻¹)
N-H Stretching	3500-3300	3390.81
C-N Stretching	1250-1000	1230.8
C=C Stretching	1667-1640	1651.9
C-S Stretching	700-600	662.07
S=O Stretching	1080-1030	1075.11
C-H Bending	1500-1300	1353.97

Melting point determination

Table 7: Melting point of drug sample.

Sample	Melting point
Silver sulphadiazine	282°C

Experimental value is in good agreement with official value thus indicating purity of the sample.

Solubility: Solubility of silver sulphadiazine was performed in various solvents like water, ethanol, chloroform, ether, ammonia solution and acetone. The results observed were as follows (Figure 3, Tables 8 and 9).

Physicochemical properties

Physical appearance: Silver sulphadiazine was found to be white crystalline powder.

Table 8: Solubility profile of the drug.

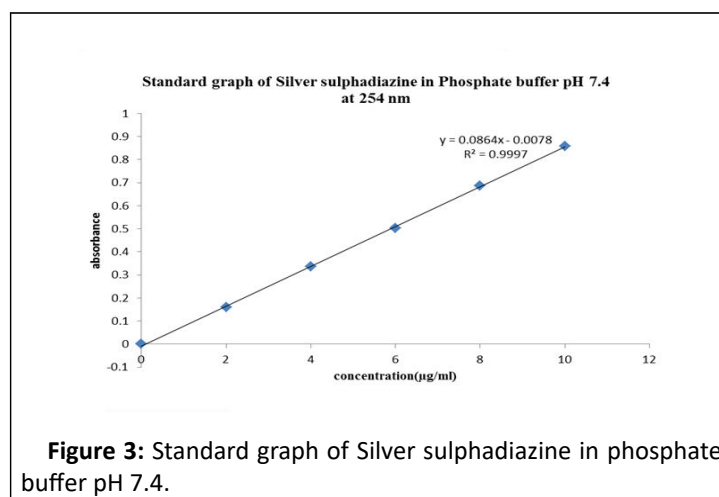
Sl. No	Solvent	Solubility of Silver sulphadiazine
1	Water	Insoluble
2	Ethanol	Partially soluble
3	Chloroform	Insoluble
4	Ether	Slightly soluble
5	Ammonia	Freely soluble
6	Acetone	Slightly soluble

Analytical methods

Table 9: The wavelength maxima of Silver sulphadiazine in different media.

Media	λ_{\max} of silver sulphadiazine (nm)
PBS pH 7.4	254

Development of calibration curve of silver sulphadiazine



Formulation of medicated nano iber: Twelve formulations of silver sulphadiazine loaded nanofibrous scaffolds were prepared by electro spinning method. Nano fibers were prepared with sodium alginate and polyvinyl alcohol in different ratios using water as solvent. All the formulations of prepared nanofiber were taken for further evaluation studies (Figures 4 and 5) [22].

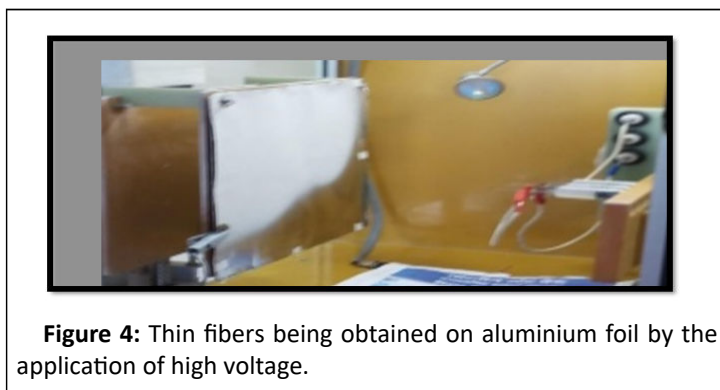


Table 10: Average fiber diameter of different formulations.

Formulation code	Average diameter (nm)
F1	114.76
F2	127.71
F3	100.68
F4	74.94
F5	107.72
F6	98.78
F7	155
F8	109.73
F9	123.03
F10	115.02
F11	118.1
F12	125.69



Evaluations of the medicated nanofibrous scaffold

Physical appearance: All the drug loaded nano fibers were found to be transparent, flexible with smooth surface (Table 10).

Morphological characterization by SEM analysis (fiber diameter)

Percentage porosity: The porosity was determined using image analysis algorithms by MATLAB. Results revealed that the porosity of all formulations varied from 36.55 to 62.48%. It was observed that formulation F4 showed maximum percentage porosity and formulation F7 showed minimum percentage porosity (Tables 11 and 12).

Table 11: Percentage porosity determination of nanofibrous scaffold.

Formulation code	Percentage porosity (%)
F1	38.96
F2	43.7
F3	45.39
F4	65.48
F5	51.28
F6	59.81
F7	35.55
F8	48.65
F9	51.59
F10	53.51
F11	44.92
F12	47.33

Degree of swelling

Table12: Swelling ability of formulations.

Formulation code	Swelling ability (%)
F1	11.23
F2	15.19
F3	22.62
F4	28.55
F5	25.33
F6	28.71
F7	15.02
F8	19.45
F9	20.18
F10	22.78
F11	20.91
F12	17.27

The degree of swelling of nanofibers plays an important role in the loading and release behavior of the drug. The swelling ability was determined by the percentage of water absorption. The results showed that the swelling ability of the nanofibrous scaffold dependent on the sodium alginate concentration. The swelling ability of the nanofiber was proportional to the sodium alginate concentration (Figures 6 and 7).

Drug entrapment estimation of medicated nanofiber

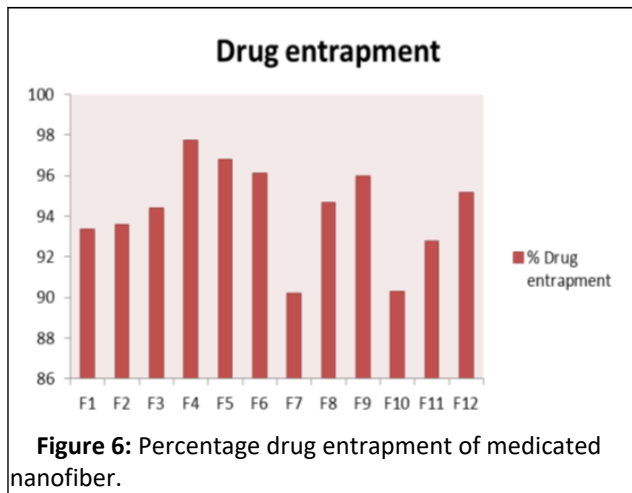


Figure 6: Percentage drug entrapment of medicated nanofiber.

Biodegradation test

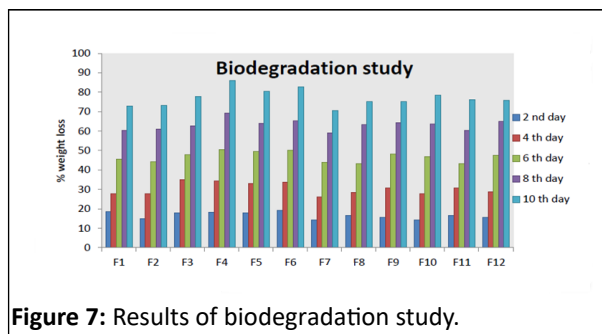


Figure 7: Results of biodegradation study.

The *in vitro* degradation study revealed that the polymers can be degraded by Lysozyme, which indicated their excellent and controllable biodegradability. Formulation F4 shows maximum biodegradability since its weight loss was 86.12 at the 10th day (Figures 8-16 and Table 13) [23].

Optimization by factorial design

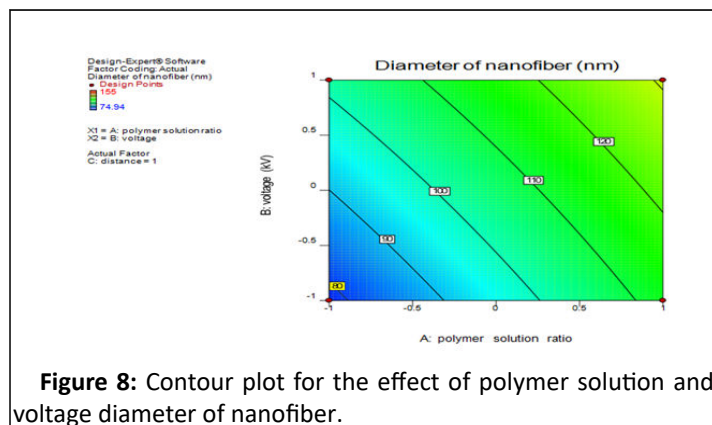


Figure 8: Contour plot for the effect of polymer solution and voltage diameter of nanofiber.

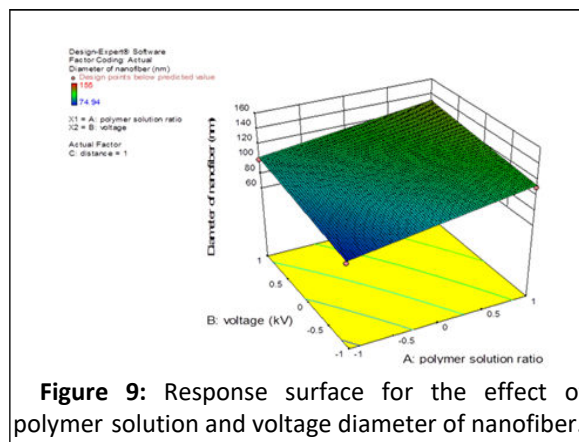


Figure 9: Response surface for the effect of polymer solution and voltage diameter of nanofiber.

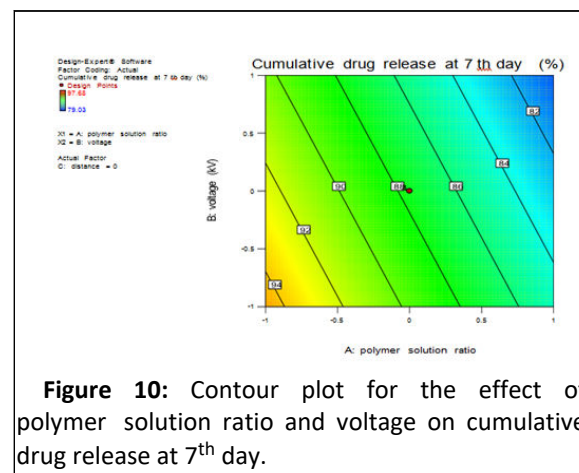


Figure 10: Contour plot for the effect of polymer solution ratio and voltage on cumulative drug release at 7th day.

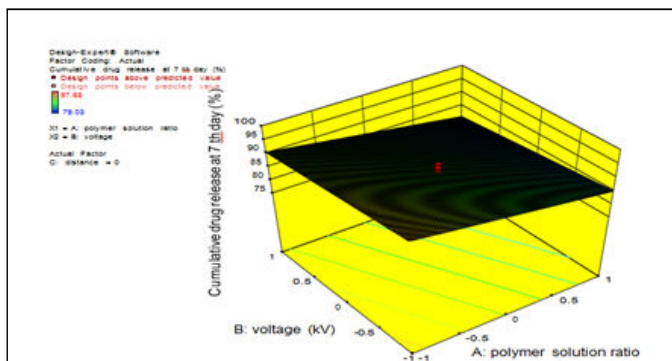


Figure 11: Response surface for the effect of polymer solution ratio and voltage on cumulative drug release at 7th day.

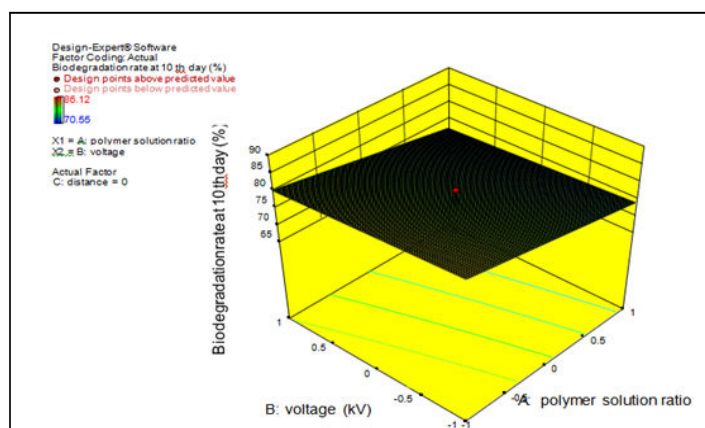


Figure 13: Response surface for the effect of polymer solution and voltage on biodegradation rate at 10th day

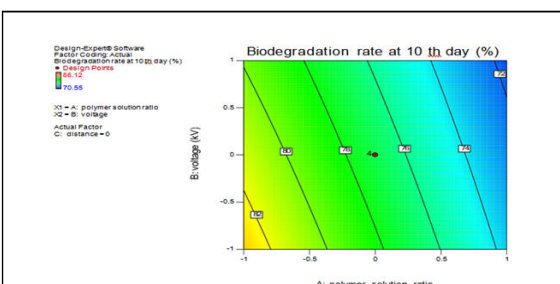


Figure 12: Contour plot for the effect of polymer solution and voltage on biodegradation rate at 10th day.

Development of the optimum batch

Table 13: Formula for optimum batch based on statistical evaluations.

Polymer solution ratio (PVA: SA)	Voltage (kV)	Distance (cm)	Diameter of nanofiber (nm)	Cumulative drug release at 7 th day (%)	Biodegradation rate at 10 th day (%)
65:35	17.027	27.94	78.38	97.79	85.76

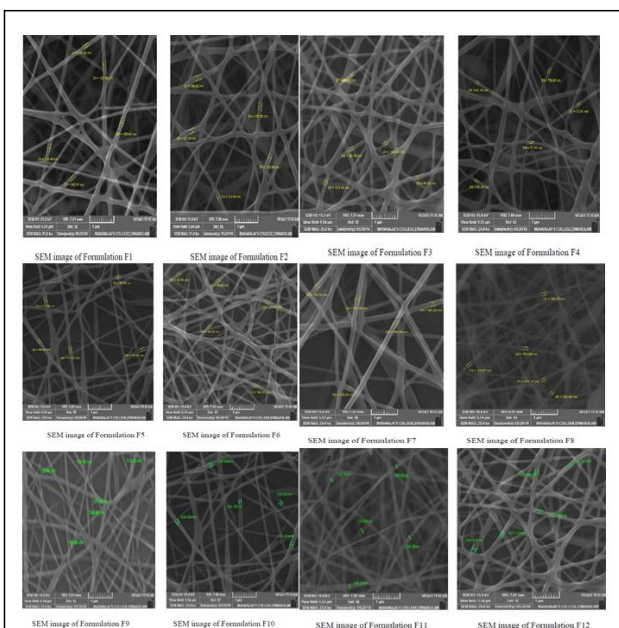


Figure 14: Morphological characterization by SEM.

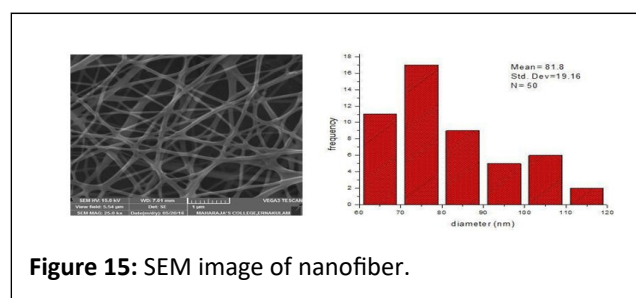


Figure 15: SEM image of nanofiber.

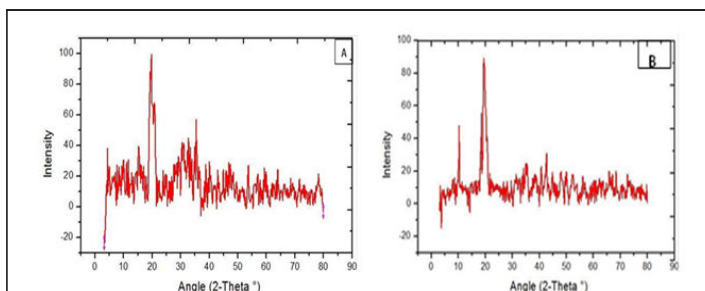


Figure 16: XRD of (A) PVA–SA composite nano fibers; (B) drug-loaded PVA–SA nano fibers.

XRD indicates that PVA could possibly interact with SA through hydrogen bonding between hydroxyl groups in PVA and the carboxyl or hydroxyl groups in Alginate. Subsequently, the

electrospinnability of SA with PVA is greatly improved (Figure 17) [24].

Thermo gravimetric analysis

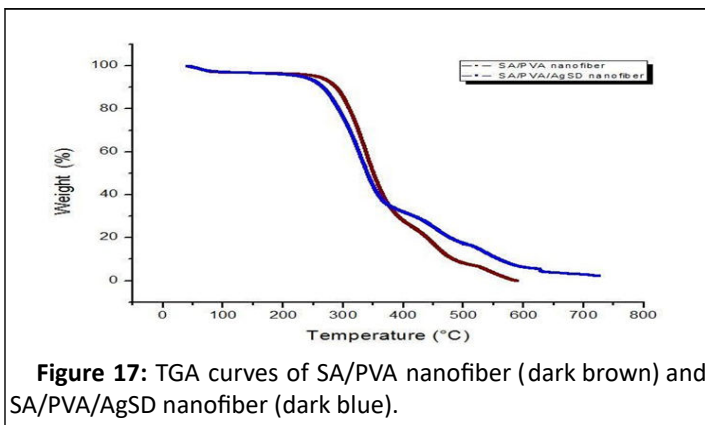


Figure 17: TGA curves of SA/PVA nanofiber (dark brown) and SA/PVA/AgSD nanofiber (dark blue).

Wound healing study



Figure 18: Wound healing study.

Estimation of drug entrapment

The percentage drug entrapment of optimized formulation was found to be 97.13% (Figures 18-20, Tables 14 and 15).

Table 14: Results of wound contraction studies.

Groups	Percentage wound contraction (%)									
	2 days	4 days	6 days	8 days	10 days	12 days	14 days	16 days	18 days	20 days
I Groups (control)	8.48 ± 1.05	13.29 ± 1.28	19.67 ± 1.42	26.54 ± 1.86	34.26 ± 1.62	44.63 ± 2.62	54.58 ± 3.08	66.72 ± 2.54	72.86 ± 2.56	90.15 ± 2.82
II Groups (std)	23.04 ± 1.35	31.12 ± 1.20	50.88 ± 1.51	65.85 ± 1.30	77.94 ± 1.71	90.99 ± 2.23	99.34 ± 0.72**			
III Groups (formulation)	34.3 ± 2.63	55.13 ± 3.12	74.06 ± 2.80	87.95 ± 1.66	99.15 ± 0.65**					

n=6 albino rats per group; values are represent mean ± SD. **p<0.01

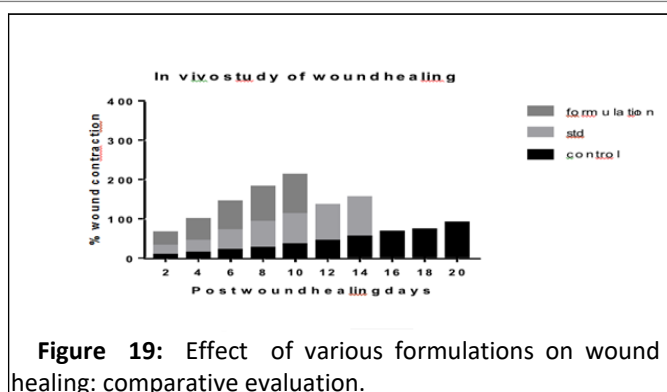


Figure 19: Effect of various formulations on wound healing: comparative evaluation.

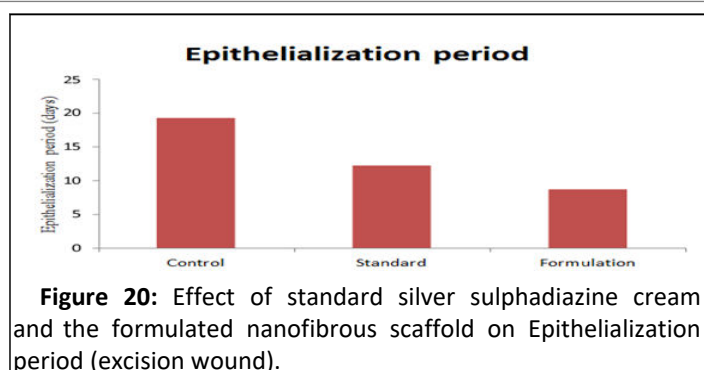


Figure 20: Effect of standard silver sulphadiazine cream and the formulated nanofibrous scaffold on Epithelialization period (excision wound).

Table 15: Results of stability study.

Parameter	Before stability	After stability
Folding endurance	451 ± 1.82	429 ± 0.84
Drug entrapment (%)	97.13	96.73

Conclusion

Medicated nanofibrous scaffold could be a good alternative to the conventional wound dressings which is painful and injurious. Which adhere to open wounds and therefore it is a good protectant providing a moist healing environment. Better patient compliance is an added advantage as it does not require repeated application. The nanofibrous scaffold could be suitably cut to fit into the wound of any size/shape and provides a sustained release of drug. The dressings are applied over and are allowed to degrade at the site giving way to new tissues. Therefore it acts as a protective and as a substrate for tissue granulation.

References

1. Abrigo M, McArthur SL, Kingshott P (2014) Electrospun Nanofibers as Dressings for Chronic Wound Care: Advances, Challenges, and Future Prospects. *Macromol Biosci* 14:772–792
2. You HJ, Han SK (2014) Cell therapy for wound healing. *J Korean Med Sci* 29:311–319
3. Robert MS, Francis X, David J, David L (2014) Spectrophotometric Identification of organic compounds. (8th edition). John Wiley and Sons Inc, New York. 464.
4. Mehta P, Sharma D, Dashora A, Sahu D, Kumar GR, et al. (2013) Design, Development And Evaluation of Lipid Based Topical Formulations of Silver Sulfadiazine for Treatment of Burns and Wounds. *Innovare J life Sci* 1:38–44
5. Fraihat SM, Bahgat KM (2014) Spectrophotometric methods for the determination of ketoconazole in pharmaceutical dosage forms. *Trop J Pharm Res* 13:1511–1514
6. Ghodekar SV, Chaudhari SP, Ratnaparakh MP (2012) Development and characterization of silver sulphadiazine emulgel for topical drug delivery. *Int J Pharm Pharm Sci* 4:305–316
7. Shalumon KT (2011) Sodium alginate/poly (vinyl alcohol)/nano ZnO composite nanofibers for antibacterial wound dressings. *Int J Biol Macromol* 49:247–254
8. Islam MS, Karim MR (2010) Fabrication and characterization of poly(vinyl alcohol)/alginate blend nanofibers by electrospinning method. *Colloids Surfaces A Physicochem Eng Asp* 366:135–140
9. Linh NTB, Min YK, Song HY, Lee BT (2010) Fabrication of polyvinyl alcohol/gelatin nanofiber composites and evaluation of their material properties. *J Biomed Mater Res B Appl Biomater* 95:184–191
10. Hotaling NA, Bharti K, Kriel H, Simon CG (2015) DiameterJ: A validated open source nanofiber diameter measurement tool. *Biomaterials* 61:327–338
11. Yarahmadi R, Zadeh AS (2015) Experimental Investigations on Electrospun Mat Production: For Use in High-Performance Air Filters. *Int J Occup Hyg* 7:110–118
12. Ghasemi-Mobarakeh L, Semnani D, Morshed M (2007) A Novel Method for Porosity Measurement of Various Surface Layers of Nanofibers Mat Using Image Analysis for Tissue Engineering Applications. *J Appl Polymer Sci* 106:2536–2542
13. Gagandeep, Tarun G, Basant M, Goutam R, Goyal AK (2014) Development and characterization of nano-fiber patch for the treatment of glaucoma. *Eur J Pharm Sci* 53:10–16
14. Freier T, Koh HS, Kazazian K, Shoichet MS (2005) Controlling cell adhesion and degradation of chitosan films by N-acetylation. *Biomaterials* 26:5872–5878
15. Don TM, Chuang CY, Chiu WY (2002) Studies on the degradation behavior of chitosan-g-poly (acrylic acid) copolymers. *Tamkang J Sci Eng* 5:235–240
16. Chaudhary AR, Ahuja BB (2014) Characterization and optimization of electrospun polyacrylonitrile (PAN) and polyvinylidene fluoride (PVDF) nanofibers. In 5th International and 26th All India manufacturing technology, design and research conference (AIMTDR 2014), IIT Guwahati, Assam, India.
17. Prajapati A, Shah D, Jani J, Singh S (2016) Fabrication of Sustained Release Matrix Tablet of Lornoxicam : Influence of Hydrophilic and Hydrophobic Polymers on the Release Rate and *In vitro* Evaluation by Full Factorial Design. *Inven J.* 2012:1–14
18. Arthanari S, Mani G, Jang JH, Choi JO, Cho YH (2014) Preparation and characterization of gatifloxacin-loaded alginate/poly (vinyl alcohol) electrospun nanofibers. *Artif Cells Nanomed Biotechnol* 44:847–52
19. Augustine R (2014) Electrospun polycaprolactone membranes incorporated with ZnO nanoparticles as skin substitutes with enhanced fibroblast proliferation and wound healing. *RSC Adv* 4:24777–24785
20. Bindu TvIH, Vidyavathi M, Kavitha K, Sastry Tp, Suresh KRv (2010) Preparation and evaluation of ciprofloxacin loaded chitosan-gelatin composite films for wound healing activity. *Int J Drug Deliv* 2:173–182
21. Li C, Fu R, Yu C, Li Z, Guan H, et al. (2013) Silver nanoparticle/chitosan oligosaccharide/poly (vinyl alcohol) nanofibers as wound dressings : a preclinical study. *Int J Nanomedicine* 8:4131–4145
22. Sadaf F, Saleem R, Ahmed M, Ahmad SI, Navaid-ul-Zafar (2006) Healing potential of cream containing extract of *Sphaeranthus indicus* on dermal wounds in Guinea pigs. *J Ethnopharmacol* 107:161–163
23. Gadekar R, Saurabh MK, Thakur GS, Saurabh A (2012) Study of formulation, characterisation and wound healing potential of transdermal patches of Curcumin. *Asian J Pharm Clin Res* 5:225–230
24. Mandal SC, Mandal M, Ghosal SK (1996) Compatibility and stability studies of matrix type transdermal drug delivery systems. *Indian Drugs* 33:511–513.